The Reaction of Peroxynitrite with Morpholine (Secondary Amines) Revisited: The Overlooked Hydroxylamine Formation

by **Michael Kirsch***[a]), **Hans-Gert Korth***[b]), **Angela Wensing**[a]), **Manfred Lehnig**[c]), **Reiner Sustmann**[b]), and **Herbert de Groot**[a])

[a]) Institut für Physiologische Chemie, Universitätsklinikum, Hufelandstrasse 55, D-45122 Essen (e-mail: michael.kirsch@uni-duisburg-essen.de)

[b]) Institut für Organische Chemie, Universität Duisburg-Essen, Universitätsstrasse 5, D-45117 Essen (e-mail: hans-gert.korth@uni-duisburg-essen.de)

[c]) Fachbereich Chemie, Universität Dortmund, Otto Hahn Strasse 6, D-44221 Dortmund

In memoriam Hanns Fischer

The reaction of peroxynitrite/peroxynitrous acid with morpholine as a model compound for secondary amines is reinvestigated in the absence and presence of carbon dioxide. The concentration- and pH-dependent formation of *N*-nitrosomorpholine and *N*-nitromorpholine as reported in three previous papers ([25][26][14]) is basically confirmed. However, ^{13}C-NMR spectroscopic product analysis shows that, in the absence of CO_2, *N*-hydroxymorpholine is, at $pH \geq 7$, the major product of this reaction, even under anaerobic conditions. The formation of *N*-hydroxymorpholine has been overlooked in the three cited papers. Additional (ring-opened) oxidation products of morpholine are also detected. The data account for radical pathways for the formation of these products *via* intermediate morpholine-derived aminyl and α-aminoalkyl radicals. This is further supported by EPR-spectrometric detection of morpholine-derived nitroxide radicals, *i.e.*, morpholin-4-yloxy radicals. *N*-Nitrosomorpholine, however, is very likely formed by electrophilic attack of peroxynitrite-derived N_2O_4. ^{15}N-CIDNP Experiments establish that, in the presence of CO_2, *N*-nitro- and *C*-nitromorpholine are generated by radical recombination. The present results are in full accord with a fractional ($28 \pm 2\%$) homolytic decay of peroxynitrite/peroxynitrous acid with release of free hydroxyl and nitrogen dioxide radicals.

1. Introduction. – Since the seminal paper of *Beckman* and colleagues [1] in which the formation of peroxynitrite/peroxynitrous acid (= oxoperoxonitrate(1−) ($ONOO^-$)/ hydrogen oxoperoxonitrate(1−) (ONOOH)) has been proposed to occur in living organisms from the diffusion-controlled reaction of endogenous superoxide radical anion ($O_2^{\bullet -}$) and nitric oxide (= nitrogen monooxide; $^\bullet NO$), the chemical and pathophysiological characteristics of this putative toxic intermediate have intensely been investigated. To date, the essential chemical characteristics of peroxynitrite in aqueous solution have been firmly established, revealing that radical processes, initiated by homolytic O−O bond cleavage to produce a fraction of $28 \pm 2\%$ free (cage-escaped) hydroxyl and nitrogen dioxide radicals (*Eqn. 1*), play a major role for its chemical reactivity [2–6].

In the absence of any substrates, nitrate is by far the major product from peroxynitrite at acidic pH, but at $pH > 6$ substantial amounts of molecular oxygen and nitrite are being produced in competition to nitrate. We have recently demonstrated that the formation of these products and the underlying kinetics in the full pH range 1–14 is

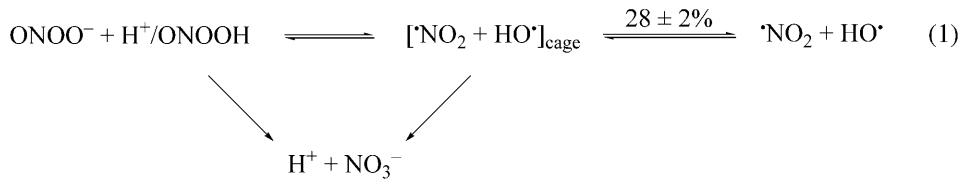

(1)

related to a complex reaction cascade following the initial release of the highly reactive HO• and NO_2• radicals [4]. In the presence of carbon dioxide, the reactivity of peroxynitrite is modulated by a relatively fast ($k = 3 - 5.8 \cdot 10^4$ M^{-1} s^{-1}) reaction with CO_2 to produce NO_2• and the carbonate radical anion, CO_3•$^-$, at a fraction of *ca.* 30–33% [7–9]. In accord with the release of strongly oxidizing radicals, peroxynitrite-mediated oxidation of organic and inorganic substrates mainly follows radical pathways.

The pathophysiological relevance of endogenously produced peroxynitrite is still a matter of debate. For the elucidation of possible biochemical pathways of peroxynitrite, a variety of model studies have been performed in the past. Reaction with typical models for biological compounds preferably leads to oxygenation (hydroxylation), nitration, and nitrosation [6][10–16]. The yields of such products, however, are generally rather low, very rarely as high as 30% relative to the amount of applied peroxynitrite. Noteworthy, yields of *ca.* 8 and 13% ('magic yields') seem to be very characteristic for a broad variety of reactants (see [4] for a collection of related references). Significantly lower yields (*ca.* 1–2%) have been observed for the peroxynitrite-dependent nitrosation of thiols [17–19] and of indole derivatives [20][21].

The peroxynitrite-induced nitrosation of 1,2-phenylenediamine (= benzene-1,2-diamine) has been contradictorily explained by an NO^+ activity of peroxynitrous acid [22] and by a homolytic pathway [23]. We have shown that peroxynitrite oxidizes tertiary amines in an initial one-electron step to generate the corresponding amine radical cations, a process which strongly indicates the intermediacy of HO• radicals [24]. In three recent studies, the reaction of peroxynitrite with secondary amines – by which cancerogenic *N*-nitrosamines may be produced – has been probed with the model compound morpholine (**MorH**) [14][25][26]. In these studies, *N*-nitrosomorpholine (**MorNO**) and *N*-nitromorpholine (**MorNO2**) have been reported as the sole products, produced in a pH-dependent manner, and with their yields (relative to peroxynitrite) in the range of the above mentioned 'magic yields' of 8 and 13%. The formation of **MorNO** and **MorNO2** was uniformly interpreted in terms of radical processes, following attack of HO• on morpholine to generate *via* N–H H-atom transfer the corresponding aminyl radical (**Mor**•).

However, as HO•-mediated H-abstraction from the methylene groups of **MorH** is also a viable process (see *Sect. 3*), and as above pH 6 substantial amounts (up to 30% at pH 9–10) of O_2 are being produced during decomposition of peroxynitrite, one would also expect the formation of *N*- and/or *C*-oxygenated (*e.g.*, hydroxylated) products because the reaction of both aminyl and C-centered radicals with O_2 is essentially diffusion-controlled (see below). Surprisingly, in none of the three above-cited studies, morpholine-based products other than **MorNO** and **MorNO2**, *e.g.*, deriving from C-centered morpholine radicals or from further transformation of initially produced **MorNO**/**MorNO2**, have been reported.

In the course of our studies on the reactivity of peroxynitrite with ubiquitous biomolecules [12][27–29], we found evidence that from secondary amines also products other than *N*-nitrosated or *N*-nitrated compounds were formed. We, therefore, reinvestigated the reaction of morpholine with peroxynitrite more closely by means of ^{13}C- and ^{15}N-NMR spectroscopy. In the present study, we show that in the presence of atmospheric or peroxynitrite-released O_2, *N*-hydroxymorpholine (**MorOH**) is a major product of this reaction, accompanied by a variety of minor oxidation products of morpholine. Detection of the intermediate morpholine-derived nitroxide radical **MorO**$^{\bullet}$ by EPR spectroscopy and ^{15}N-CIDNP-NMR experiments further supports a radical pathway of peroxynitrite-mediated oxidations of secondary amines in the absence and presence of carbon dioxide.

2. Results. – *Carbon Dioxide-Free Conditions. Formation of* N-*Nitrosomorpholine and* N-*Nitromorpholine.* In previous studies on peroxynitrite-mediated nitrosation and nitration of morpholine (**MorH**), both reactants were either applied in equimolar amounts or moderate concentration ratios not exceeding tenfold excesses of the one compound over the other [14][25][26]. However, although the rates of reaction of HO$^{\bullet}$ with secondary amines and cyclic ethers are close to the diffusion-controlled limit ($k = 10^9 - 10^{10}$ M^{-1} s^{-1}; see the numerous data in the *NIST* database [30]), effective trapping of peroxynitrite-released HO$^{\bullet}$ radicals would require higher concentrations of **MorH** because HO$^{\bullet}$ attack on its own precursor peroxynitrite is also a diffusion-controlled process [$k(\mathrm{HO}^{\bullet} + \mathrm{ONOO}^{-}) = 4.8 \cdot 10^9$ M^{-1} s^{-1}][31], *i.e.*, may compete efficiently with attack on **MorH** at low [**MorH**]/[peroxynitrite] ratios. Therefore, in our experiments, we varied the [**MorH**]/[peroxynitrite] ratio up to a limiting value of 300 : 1 (see below). *N*-Nitrosomorpholine (**MorNO**) and *N*-nitromorpholine (**MorNO2**) were initially identified by GC/MS, capillary-zone electrophoresis (CE), and thin-layer chromatography (TLC) by comparison with authentic material. Quantification was performed by CE. The detection limits of our CE instrument were *ca.* 2.5 μM for **MorNO** and *ca.* 15 μM for **MorNO2**.

At a fixed concentration of 1 mM peroxynitrite, **MorNO** formation at pH 7.5 and 37° could not be detected by CE at **MorH** concentrations lower than 5 mM (*Fig. 1*); about 25 μM **MorNO** was found in the presence of 10 mM **MorH**, the formation of **MorNO** increased exponentially with increasing morpholine concentration, approaching a plateau value of *ca.* 77 μM at 300 mM morpholine.

At higher concentrations of peroxynitrite (≥ 2 mM), formation of **MorNO2** was also detected. At pH 7.5, production of both **MorNO** and **MorNO2** is strictly proportional ($r^2 = 0.998$) to the amount (1–10 mM) of added peroxynitrite (*Fig. 2*). The relative yields of **MorNO** and **MorNO2**, as derived from the slope of the regression line, corresponded to *ca.* 7.2 and 1.6 mol-%, respectively, of the initial amount of peroxynitrite. The latter value agrees fully with the maximum yield of **MorNO2** reported by *Uppu*, *Squadrito*, and co-workers for 2 mM peroxynitrite and 5 mM **MorH** at pH 9 [25]. It must be emphasized that under the applied conditions, **MorNO2** is not produced from further oxidation of **MorNO** by peroxynitrite, as revealed by blank experiments where authentic **MorNO** (0.1–1 mM) was allowed to react with excess peroxynitrite (1–10 mM) (data not shown).

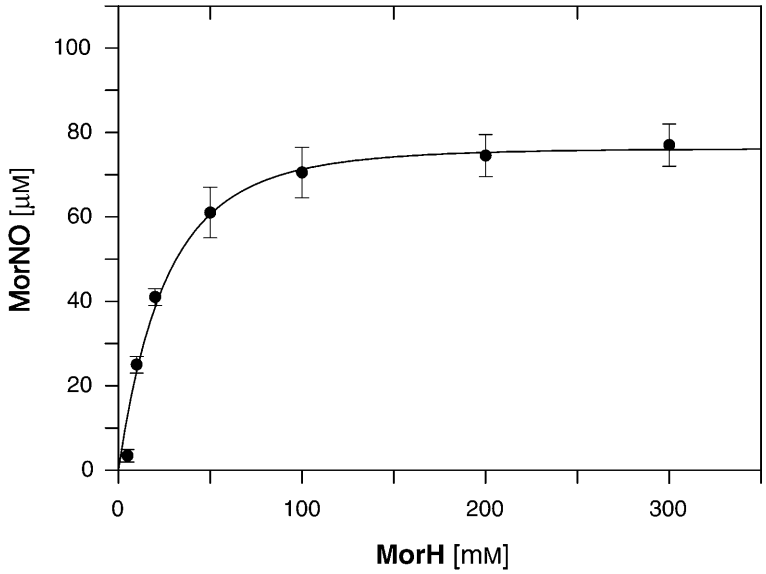

Fig. 1. *Dependence of* N-*nitrosomorpholine production from peroxynitrite* (1 mM) *on the concentration of morpholine at pH 7.5*. [Phosphate buffer] = 50 mM; *T* 37°. The solid line is a fit of a single exponential to the data points.

As reported previously, the production of both **MorNO** and **MorNO2** is strongly pH-dependent [14][25][26]. At pH 6, formation of **MorNO** from 300 mM **MorH** and 1 mM peroxynitrite was undetectable by CE (*Fig. 3*), *i.e.*, $\leq$2.5 μM. With increasing pH, **MorNO** formation increased to reach a maximum value of *ca.* 140 μM (14%) at pH 10. Above this pH, the yield of **MorNO** decreased slightly. The relative maximum yield at pH 10 is close to the maximum yield of 12% at 25° given by *Uppu*, *Squadrito*, and co-workers [25] for a 2.5 : 1 [**MorH**]/[peroxynitrite] ratio.

Differently, *Ohshima* and co-workers [26] reported only a **MorNO** yield of 5% at pH 9 from an equimolar (1 mM) ratio of the reactants. Therefore, the dependence of **MorNO** formation on the concentration of **MorH** was also determined at pH 11 (*Fig. 4*). At 1 mM equimolar concentrations, a yield of *ca.* 85 μM (8.5%) of **MorNO** was found, which increased to a maximum value of *ca.* 138 μM (*ca.* 14%) at 50 mM morpholine. At the limiting concentration of 300 mM **MorH**, the yield of **MorNO** had slightly decreased to 123 $\pm$ 9 μM (*ca.* 12%).

Since at high **MorH** concentrations ($\geq$10 mM), our solutions cannot be considered to be true phosphate buffer systems, but rather represent amine/ammonium buffers, we performed exploratory experiments to check whether **MorNO** formation would be affected by the concentration of the phosphate buffer (*Fig. 5*). Clearly, **MorNO** production from 1 mM peroxynitrite and 200 mM **MorH** is virtually independent on phosphate buffer concentration up to 250 mM, but drops to about one-half at 750 mM. This effect yet has to be explored.

Ohshima and co-workers [26] have shown for a variety of secondary amines that *N*-nitrosation by peroxynitrite seems to be a general process and that the yields of *N*-

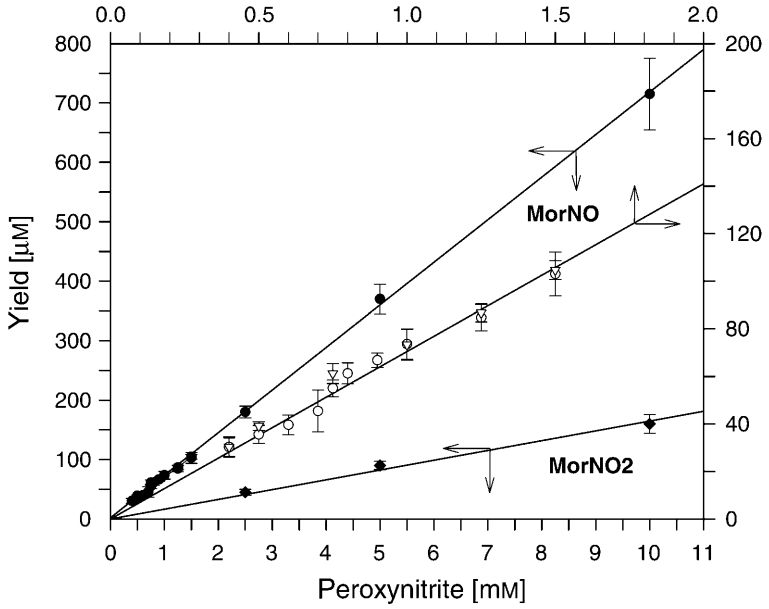

Fig. 2. *Dependence of* N-*nitrosomorpholine* (upper and middle trace) *and* N-*nitromorpholine production* (lower trace) *from 300 mM morpholine on the concentration of peroxynitrite.* [Phosphate buffer] = 50 mM; T 37°. The middle trace is the expansion of the **MorNO** data points at low peroxynitrite concentrations. Open circles: solutions treated with DTPA (= diethylenetriaminepentaacetic acid = *N*,*N*-bis{2-[bis(carboxymethyl)amino]ethylglycine); open triangles: solutions treated with *Chelex*.

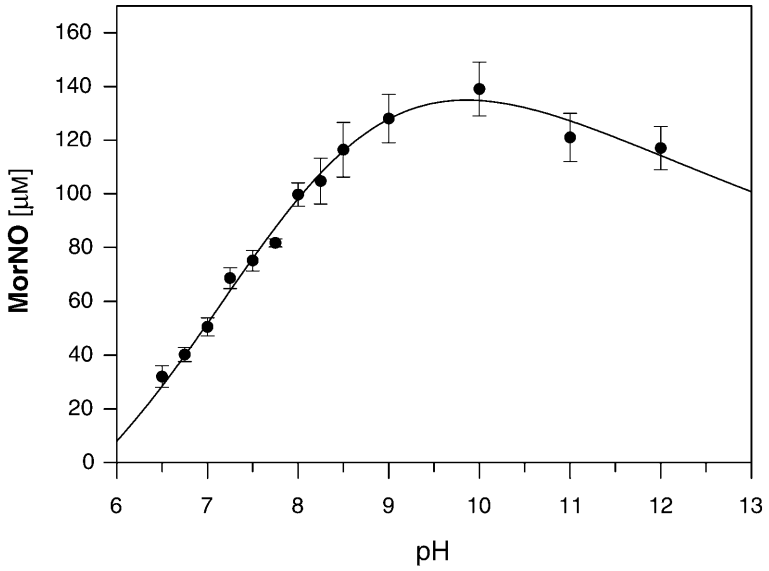

Fig. 3. *pH-Dependence of* N-*nitrosomorpholine production from 1 mM peroxynitrite and 300 mM morpholine.* [Phosphate buffer] = 50 mM; *T* 37°.

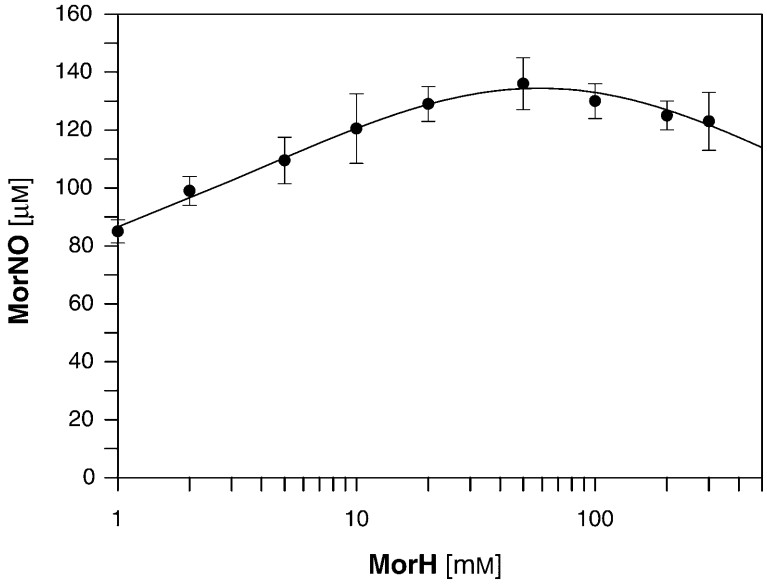

Fig. 4. *Dependence of* N-*nitrosomorpholine production from 1 mM peroxynitrite on the concentration of morpholine at pH 11. T* 37°.

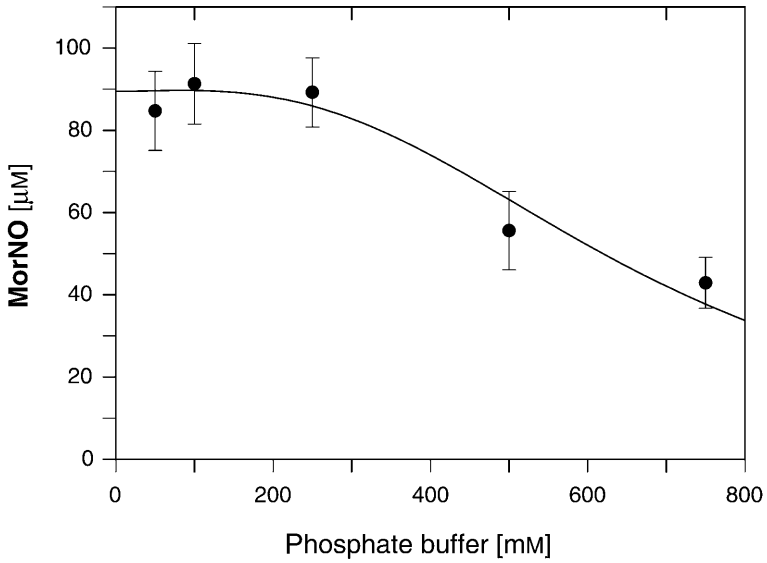

Fig. 5. *Effect of phosphate buffer concentration on* N-*nitrosomorpholine formation from 1 mM peroxynitrite and 200 mM morpholine.* At pH 7.5, *T* 37°.

nitrosoamines and *N*-nitroamines depend on the pK_a of the corresponding ammonium ion. This was confirmed by reaction of buffered solutions of 'diethanolamine' (=2,2′-iminobis[ethanol]), piperidine, and pyrrolidine (300 mM each) with 1 mM peroxynitrite.

At pH 7.5, out of these amines, only diethanolamine gave yields of the related *N*-nitrosoamine (14.3 ± 1.9 μM, 1.4%) exceeding our detection limit. At pH 10, where morpholine ($pK_a = 8.36$) gave *ca.* 13.5% **MorNO**, the *N*-nitrosoamines of diethanolamine, piperidine, and pyrrolidine were produced in yields of 5.9, 0.5, and 0.5%, respectively, from 300 mM of the amine and 10 mM peroxynitrite (*Table 1*). The yields of the *N*-nitrosoamines correlate with the pK_a values of the corresponding ammonium ions of the amines (the plot of log[*N*-nitrosoamine] *vs.* pK_a is reasonably linear), showing that access to the unshared electron pair at the N-atom is essential for the nitrosation reaction. Note that our yields of **MorNO** and *N*-nitrosopyrrolidine were about twice as high as the yields reported by *Ohshima* and co-workers [26] for equimolar ratios of the reactants.

Table 1. N-*Nitrosoamine Production from Reaction* (3 h) *of Peroxynitrite* (10 mM) *with Various Secondary Amines* (300 mM each) *in Potassium Phosphate Buffer* (50 mM; pH 10) *at 37°*

Amine	*N*-Nitrosoamine [μM][a])	$pK_a(R_2NH_2^+)$
Morpholine	1345 ± 38 (13.5)	8.36
Diethanolamine[b])	588 ± 15 (5.9)	8.88
Piperidine	52 ± 2 (0.5)	11.22
Pyrrolidine	49 ± 1 (0.5)	11.27

[a]) Percentage yields relative to applied peroxynitrite given in parentheses. [b]) Systematic name: 2,2′-iminobis[ethanol].

^{13}C-NMR Experiments. ^{13}C-NMR Spectra were recorded after rapid mixing at 20° of deoxygenated and CO_2-free solutions of **MorH** (300 mM) in phosphate buffer pH 7.5 with alkaline solutions of peroxynitrite to give a 10 mM final concentration. (The [**MorH**]/[peroxynitrite] ratio 30 : 1 was chosen to avoid complete suppression of peroxynitrite-derived O_2 production). The spectra accumulated within the first 15 min after mixing revealed the formation of a variety of products having resonances exclusively in the δ 40–70 and 160–170 ppm range (*Fig. 6, a*).

In accord with the short lifetime of peroxynitrite at this pH ($t_{1/2} \approx 4$ s), product formation is essentially complete when the first spectrum can be recorded. By comparison (spiking) with the mixture of authentic material (see *Exper. Part*), **MorNO2**, **MorNO**, and **MorOH** were identified as products (*Table 2*), formed in an approximate 1 : 2.7 : 3.6 molar ratio. Hence, **MorOH** is in fact the major product from peroxynitrite and **MorH** under these conditions. The **MorNO**/**MorNO2** ratio corresponded reasonably well with the 4.4 : 1 ratio as determined by CE for a reaction temperature of 37°. Byproducts of similar signal intensity had resonances at δ 40.0, 54.3, 62.2, 65.3, and 170, minor signals were detected at δ 39.6, 45.5, 48.5, 59.4, 66.1, 66.3, and 162.1. A DEPT spectrum showed that *all* resonances in the δ 30–70 range are due to CH_2 groups, establishing that no significant amounts of stable mono-substituted oxidation products (*e.g. C*-nitro, *C*-nitroso, or *C*-hydroxy compounds) were formed. On partial decoupling, the signals at δ 162 and 170 were both split into *doublets*, *i.e.*, they were certainly due to aldehyde groups.

From the relative intensity of the sum of the δ 35–70 resonances, a **MorH** conversion of roughly 8% (the 'magic yield') was estimated, in reasonable agreement with the

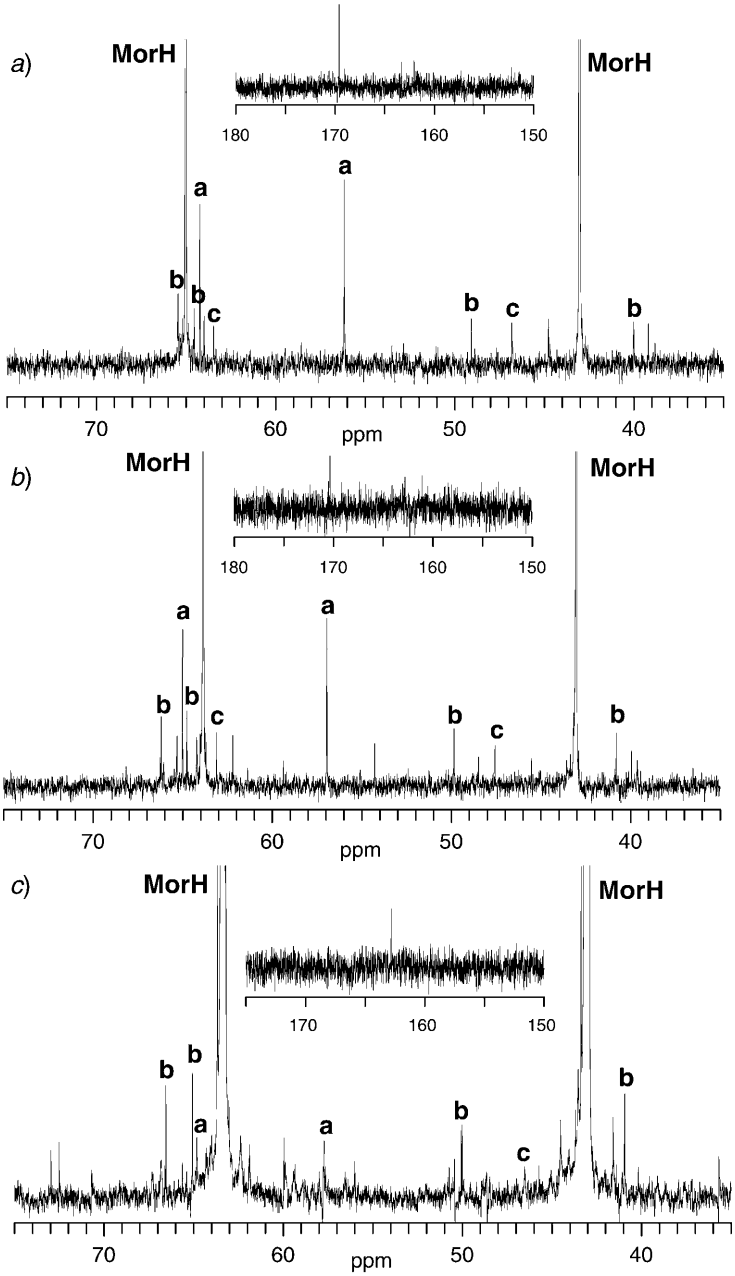

Fig. 6. *^{13}C-NMR Spectra of products from reaction of peroxynitrite with morpholine in phosphate buffer at* a) *pH 9.0*, b) *pH 7.4*, *and* c) *pH 4.8*. [Peroxynitrite] = 10 mM, [**MorH**] = 300 mM, [phosphate buffer] = 50 mM; *T* 25°. Spectra are sums of four spectra recorded in 15-min intervalls after mixing of the reactants. Labels: **a** = **MorOH**, **b** = **MorNO**, **c** = **MorNO2**.

Table 2. *^{13}C-NMR Chemical-Shift Data* (rel. to $SiMe_4$ (= 0 ppm))

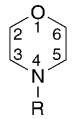	Position	δ [ppm]			
		Acetate buffer pH 4.5[a])	Phosphate buffer pH 7.5[b])	Phosphate buffer pH 9.0[b])	CD_3CN[c])
MorH (R = H)	C(3), C(5)	43.1	43.1	43.1	44.2
	C(2), C(6)	63.4	63.5	65.0	64.5
MorNO (R = NO)	C(3)[d])	50.0	49.9	49.1	50.6
	C(2)[d])	66.5	66.2	65.4	66.8
	C(6)[e])	65.1	64.8	64.6	66.2
	C(5)[e])	41.6	41.0	40.0	41.0
MorNO2 ($R = NO_2$)	C(2), C(6)	46.3	46.6	46.8	49.3
	C(3), C(5)	n.r.[f])	63.3	63.6	66.9
MorOH (R = OH)	C(3), C(5)	57.7	56.9	56.2	59.6
	C(2), C(6)	64.8	65.0	64.2	65.7

[a]) From the $NaNO_2 + H_2O_2$ reaction. [b]) From the reaction with preformed peroxynitrite. [c]) ^{15}N-labelled compounds, from electrolysis of $^{15}NO_2^-$. [d]) *anti* to N=O; J(C,N) = 5.6. [e]) *syn* to N=O. [f]) Not resolved, covered by **MorH** resonance.

yields of **MorNO**/**MorNO2** determined by CE (*cf. Fig. 2*). The relative intensity of all NMR signals did not vary noticeably within 2 h, thus, further transformation of the products, *e.g.*, by hydrolysis, is slow. No further attempts were made to elucidate the structures of the by-products, but the absence of additional ^{15}N-NMR resonances other than those of **Mor^{15}NO**, **Mor^{15}NO2**, $^{15}NO_2^-$, and $^{15}NO_3^-$, when this experiment was performed with (^{15}N)peroxynitrite (data not shown), ruled out significant incorporation of peroxynitrite-derived N-atoms.

At pH 9, product formation was complete after 15 min, where the overall conversion of **MorH** had increased to *ca.* 12%, and the relative yields of **MorOH**, **MorNO**, and **MorNO2** had changed in favor of **MorOH** to an approximate ratio of 4.4 : 2.2 : 1 (*Fig. 6,b*). The enhanced production of **MorOH** compared to **MorNO**, and **MorNO2** is in line with the fact that at this pH substantial amounts of O_2 are produced from peroxynitrite. Noticeably, less by-products than at pH 7.5 were formed, major peaks were detected at δ 39.2, 44.8, 64.0, and 169.6. In addition to the δ 162 and 170 aldehyde resonances already observed at pH 7.5, further carbonyl resonances were found at δ 163.3 and 166.3.

Because at pH < 6 peroxynitrite decomposes completely within a few seconds, peroxynitrite was generated at pH 4.8 *in situ* from the reaction of $^{15}NO_2^-$ with hydrogen peroxide in acetate buffer in the presence of 300 mM **MorH**. The ^{13}C-NMR spectra recorded immediately after mixing of the reactants revealed a low conversion of **MorH**. A plethora of new resonances was observed (*Fig. 6,c*). From the relative signal intensities of the CH_2 groups in the δ 30–70 range, a total conversion of **MorH** of *ca.* 3% after 1 h was estimated, with **MorNO** being the major product (*ca.* 1.2%). **MorOH** was formed to a smaller extent (about one-fourth of [**MorNO**]), in agreement with the low production of oxygen at this pH [4]. **MorNO2** could not be detected. This was confirmed by the ^{15}N-NMR spectrum, in which only **MorH** (in natural abundance of ^{15}N), $^{15}NO_3^-$, and **Mor^{15}NO** were detected (data not shown). The **Mor^{15}NO** signal

grew slowly with time, indicating additional nitrosation of **MorH** *via* the common electrophilic HNO_2/N_2O_3 and/or $HOONO_2$ pathways.

Effect of Hydroxyl-Radical Scavengers. To substantiate the involvement of HO• radicals in the *N*-nitrosation process, the influence of compounds commonly regarded as typical hydroxyl-radical scavengers, namely benzoic acid, mannitol, ethanol, and DMSO (200 mM each) on reaction of peroxynitrite (1 mM) with morpholine (50 mM) was studied (*Table 3*). As can be seen, formation of **MorNO** was partially reduced in the presence of these compounds, with DMSO being the most effective trap.

Table 3. *Effect of Hydroxyl-Radical Scavengers* (200 mM each) *on the Production of* N-*Nitrosomorpholine from Reaction of Peroxynitrite* (1 mM) *with Morpholine* (50 mM) *in Potassium Phosphate Buffer* (50 mM, pH 7.5) *at 37°*

Scavenger	*N*-Nitrosoamine [μM]	ΔYield [%]	k(HO• + scavenger)[a]) [10^9 M^{-1} s^{-1}]
None	64.9 ± 3.9	–	
Benzoic acid	55.1 ± 2.7	−15	3.30
Ethanol	47.2 ± 4.3	−27	1.80
Mannitol	40.5 ± 3.9	−38	1.85
DMSO	38.3 ± 2.3	−41	7.0

[a]) Data from [30].

Influence of Azide on N-*Nitrosomorpholine Formation*. The influence of the azide ion on the formation of nitrosated products is commonly used to underline the action of N_2O_3 as nitrosating species ([32] and ref. cit. therein). In our system (1 mM peroxynitrite, 50 mM **MorH**), azide concentrations in the millimolar range had to be applied to reduce the peroxynitrite-dependent **MorNO** production significantly (*Fig. 7*). The yield of **MorNO** was diminished roughly linearly ($r^2 = 0.989$) with increasing azide concentration and was completely abolished at ≥ 5 mM N_3^-. *Goldstein* and *Czapski* [33] reported that azide reacts with peroxynitrite in the presence of CO_2. To verify whether a similar reaction would occur also in the absence of CO_2, the yields of nitrite and nitrate under the above conditions were determined. In view of the fact that N_3^- reacts with both N_2O_3 and N_2O_4 (*Eqns. 2* and *3*) [32] and assuming that production of NO_2^- from peroxynitrite proceeds *via* hydrolysis of intermediately formed N_2O_3 (*Eqn. 4*) [4], the decrease of the NO_2^- yield was expected to correlate with the consumption of N_3^-. However, contrary to this expectation, formation of NO_3^- but not of NO_2^- was found to be diminished by added azide (*Fig. 8*). Rather, at lower azide concentrations, nitrite production was even slightly enhanced. Noteworthy, the combined $NO_2^- + NO_3^-$ yield was continuously diminished to a limiting percentage of 17.5% at high concentration of N_3^-. This observation strongly suggests a partial conversion of peroxynitrite to nonionic/nonhydrolyzable N-products, most reasonably N_2 and/or N_2O. This result favors the view that the HO• radicals produced from peroxynitrite had reacted with N_3^- ($k(HO^\bullet + N_3^-) = 1.2 \cdot 10^{10}$ M^{-1} s^{-1}) [30] (see *Sect. 3*).

$$N_3^- + N_2O_3 \rightarrow N_2 + N_2O + NO_2^- \quad (2)$$

$$N_3^- + N_2O_4 \rightarrow N_2 + N_2O + NO_3^- \quad (3)$$

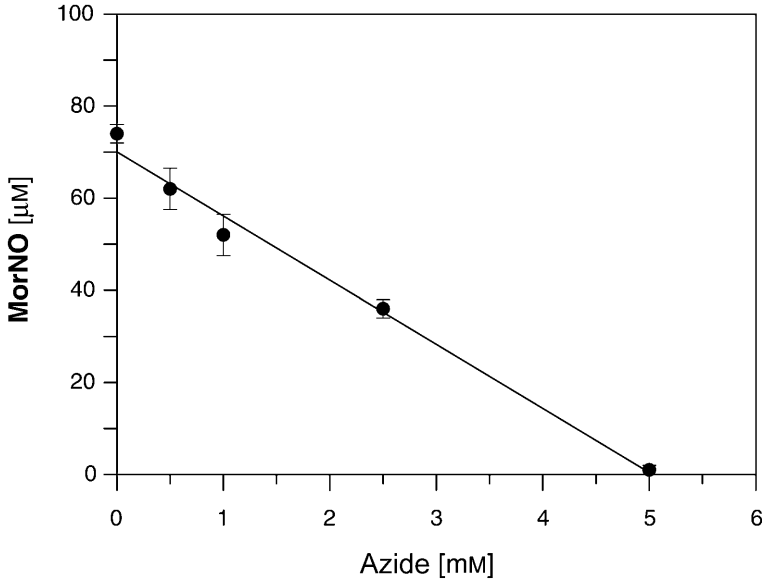

Fig. 7. *Effect of azide on* N-*nitrosomorpholine formation from 1* mM *peroxynitrite and 300* mM *morpholine at pH 7.5. T* 37°.

$$N_2O_3 + H_2O \rightarrow 2\ NO_2^- + 2\ H^+ \quad (4)$$

Formation of Hydrogen Peroxide. Nitrosation of secondary amines by peroxynitrite might, in principle, be expected to proceed also *via* a direct, nonradical (electrophilic) pathway. In such a case, production of H_2O_2 is expected, which should correlate with the production of **MorNO** in a 1:1 stoichiometry (*Eqn. 5*).

$$R_2NH + ONOO^-/ONOOH \rightarrow R_2NN{=}O + HOO^-/H_2O_2 \quad (5)$$

The base level of H_2O_2 in our peroxynitrite stock solution was found to be 4.2 ± 0.3 μM (0.58 mol-%) at all selected pH values (data not shown). After reaction of peroxynitrite (1 mM) with morpholine (300 mM) in the pH range 5–10, a significant increase of the H_2O_2 level between pH 5 and 8 was found, with a maximum yield of *ca.* 40 μM (4% relative to peroxynitrite, corrected for nitrite base level) at pH 6 (*Fig. 9*). From inspection of *Fig. 9*, it becomes obvious that the yields of **MorNO** and H_2O_2 are uncorrelated, which, in combination with the concentration dependence of **MorNO** formation (see above), largely rules out the contribution of an electrophilic nitrosation process. Noteworthy, at pH 10, peroxynitrite-mediated formation of H_2O_2 was completely abolished.

Formation of Nitric Oxide. By means of our FNOCT methodology [34–36] (FNOCT = fluorescent nitric oxide cheletropic trap), an accumulated production of 20.4 ± 3.3 μM $NO^{\bullet}$ was detected from decay of 5 mM peroxynitrite at pH 7.5, corresponding to a yield of 0.4%. It should be noted, however, that at this pH *ca.* 17% of O_2 is released from peroxynitrite [4], which might have masked a higher production of $NO^{\bullet}$ due to competitive autoxidation to $^{\bullet}NO_2$.

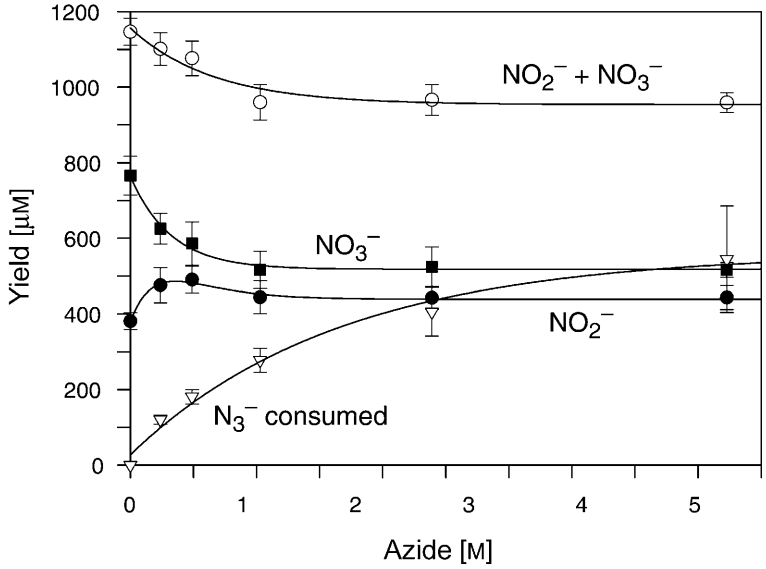

Fig. 8. *Effect of azide on the formation of nitrite and nitrate from 1.2 mM peroxynitrite at pH 7.5. T* 37°.

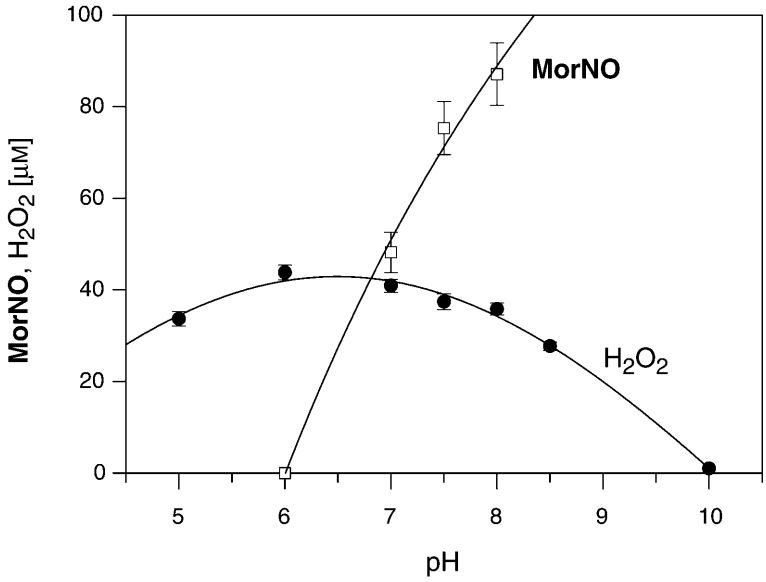

Fig. 9. *pH Dependence of hydrogen peroxide* (●) *and* **MorNO** (□) *formation from decomposition of 1 mM peroxynitrite in the presence of 300 mM morpholine.* Values corrected for 4.2 μM base level of H_2O_2. *T* 37°.

EPR Spectroscopic Experiments. The foregoing results confirm the view [14][25][26] that product formation is initiated by attack of peroxynitrite-released

$HO^{\bullet}$ radicals on **MorH** to produce the corresponding N- and/or C-centered radicals as intermediates (see *Sect. 3*). Direct EPR-spectroscopic detection of such radicals is hampered by their high reactivity (their bimolecular self-decay can safely be assumed to be diffusion-controlled [37]) in relation to the relatively slow rate of formation. Most previous attempts to detect radical intermediates from decaying peroxynitrite, therefore, utilized EPR spin-trapping techniques [38–40]. Although radical production from peroxynitrite was in fact indicated in such experiments, ambiguity generally remained with regard to the nature of the initially released radicals. As aminyl, α-aminoalkyl, and α-alkoxyalkyl radicals all react rapidly ($k \geq 10^9$ M^{-1} s^{-1}) [41] with O_2, we expected that the putative morpholine-derived aminyl radical (**Mor**$^{\bullet}$) would finally produce the corresponding morpholine-derived nitroxide radical (**MorO**$^{\bullet}$), similarly to what has been observed for other secondary amines [42][43]. In fact, after rapid mixing of a solution of **MorH** (300 mM) with peroxynitrite (5 mM final concentration) in phosphate buffer at pH 7.5, the growth of the known EPR spectrum of **MorO**$^{\bullet}$ [44][45] could be monitored (*Fig. 10*, *a*).

This EPR spectrum shows the interesting feature of an *alternating linewidth effect*; *i.e.*, at the applied temperature (20°), six of the 15 hyperfine lines expected if the four H_β atoms are assumed to be equivalent are broadened beyond detection due to a conformational *chair-twist* interconversion of the six-membered ring at an 'intermediate' rate ($k = 1.2 \cdot 10^8$ s^{-1}, according to simulation).

The EPR spectrum could also be recorded, with a reduced signal intensity, under anaerobic conditions, confirming some release of O_2 from peroxynitrite at this pH. In accord with the increased production of O_2 at alkaline pH, a more intense EPR spectrum was recorded at pH 10.5. At pH 4.5, where O_2 production is low, signals of **MorO**$^{\bullet}$ could no longer be detected. When octadeuterated morpholine (**D$_8$MorH**; 95% D) was employed in a similar experiment, a spectrum corresponding to an approximate 'rapid exchange' of the axial and equatorial deuterium atoms on the spectrometer's time scale was observed, due to the smaller difference of the related hyperfine splittings (*Fig. 10*, *b*). The EPR signal intensity of the **MorO**$^{\bullet}$ radical increased strongly within the first minute after mixing of the reactants, followed by a slower decay with a half-life of *ca.* 2.5 min at 20°.

Presence of Carbon Dioxide. Influence of Hydrogen Carbonate on Product Formation. The decomposition of peroxynitrite in the presence of HCO_3^-/CO_2 at 2.5 and equimolar [**MorH**]/[peroxynitrite] ratios has been studied by *Uppu*, *Squadrito*, and co-workers [25], and *Ohshima* and co-workers [26], respectively, showing that HCO_3^-/CO_2 enhances **MorH** nitration over nitrosation at pH ≥ 7. Therefore, we studied the peroxynitrite-mediated formation of **MorNO** and **MorNO2** at pH 7.5 and 37° only at the limiting value of 300 mM morpholine (*Fig. 11*). At 1 mM HCO_3^-, the yield of **MorNO** was essentially the same (78 μM) as in the absence of HCO_3^-, but formation of **MorNO2** had increased to *ca.* 32 μM. With increasing HCO_3^-concentration, the yield of **MorNO** was slightly (*ca.* 29%) decreased to a constant level of 55 μM, whereas production of **MorNO2** was strongly enhanced to reach a plateau value of *ca.* 103 μM at 25 mM HCO_3^-. Control experiments confirmed that **MorNO2** was not formed from further reaction of **MorNO** (0.1–1 mM) with peroxynitrite (1–10 mM) in the presence of HCO_3^- (25–50 mM) (data not shown), similar to what was found in the absence of HCO_3^-/CO_2.

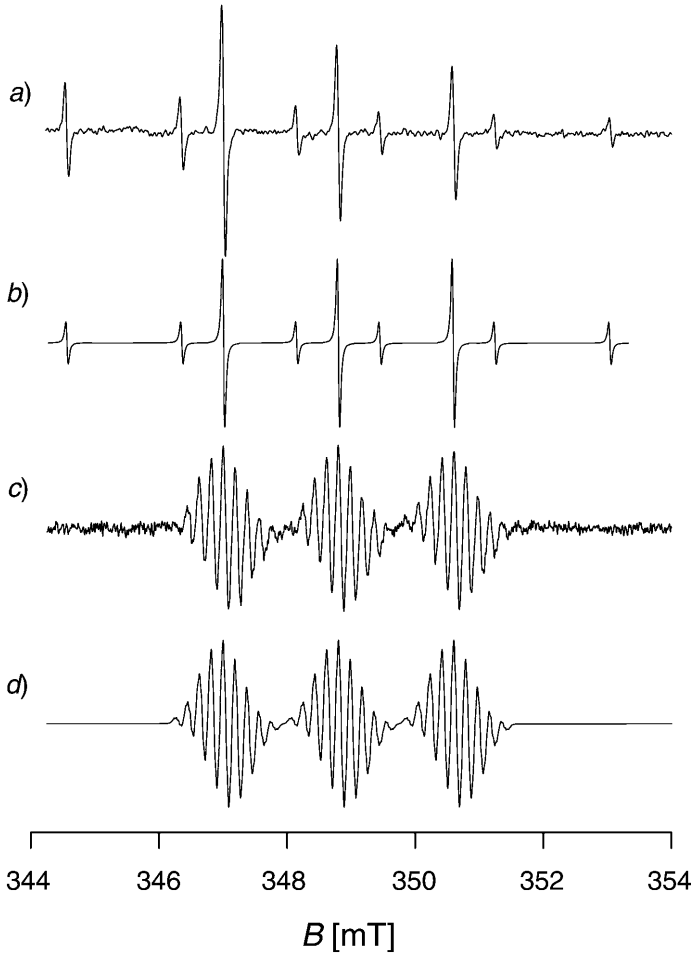

Fig. 10. *EPR Spectra of the (D$_8$)morpholin*-N-*yloxy radical* (**D$_8$MorO$^\bullet$**) *from decomposition of peroxynitrite in phosphate buffer in the presence of (D$_8$)morpholine:* a) *Experimental spectrum of morpholin*-N-*yloxy* (**MorO$^\bullet$**) (pH 7.4). b) *Simulated exchange-broadened spectrum for a ring-inversion rate of* $1.2 \cdot 10^8$ s^{-1} (hyperfine splittings: a(N) = 1.805, $a(H_{\beta,ax})$ = 2.46 and 0.0 (2 H), $a(H_{\beta,eq})$ = 0.0 and 2.46 (2 H), and $a(H_\gamma)$ = 0.03 (4 H) mT; g = 2.00576). c) *Experimental spectrum of the (D$_8$)morpholin*-N-*yloxy radical* (**D$_8$MorO$^\bullet$**) (pH 10.6). d) *Simulated exchange-broadened spectrum for a ring-inversion rate of* $8.8 \cdot 10^8$ s^{-1} (hyperfine splittings: a(N) = 1.801, $a(D_{\beta,ax})$ = 0.367 and 0.0 (2 D), $a(D_{\beta,eq})$ = 0.0 and 0.367 (2 D), $a(D_\gamma)$ = 0.02 (4 D) mT; g = 2.00576). [**MorH**] or [**D$_8$MorH**] = 300 mM, [peroxynitrite] = 5 mM; T 20°

Morpholine-Dependent Product Formation. In the presence of 25 mM HCO_3^-, formation of **MorNO2** from the reaction of 1 mM peroxynitrite with morpholine at pH 7.5 could only be detected above 2 mM **MorH**. **MorNO2** production increased exponentially with [**MorH**] to level off at *ca.* 95 μM at morpholine concentrations ≥ 100 mM (*Fig. 12*). **MorNO** formation was evident only at [**MorH**] ≥ 10 mM, reaching a maximum value of *ca.* 63 μM at 300 mM morpholine. The yields of **MorNO2**/**MorNO** were somewhat affected when the solutions were additionally bubbled with air/CO_2 95 : 5% (*Fig.*

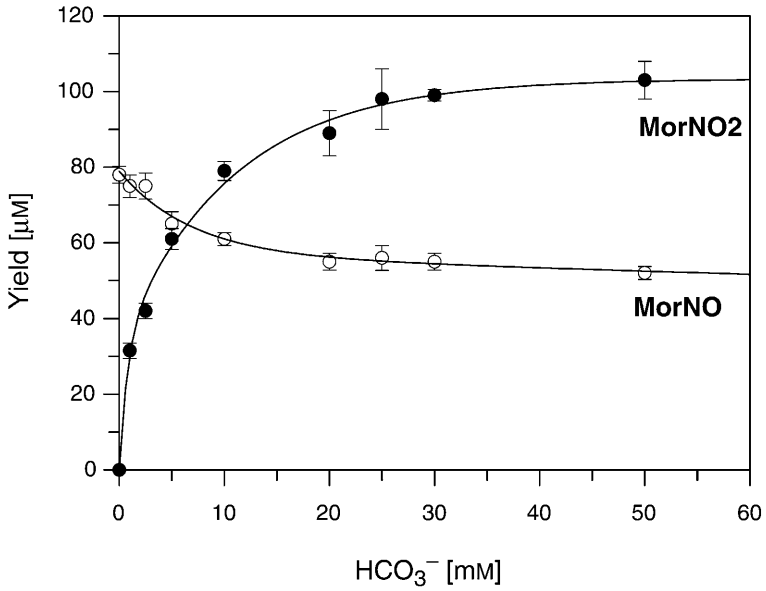

Fig. 11. N-*Nitroso- and* N-*nitromorpholine formation from 1 mM peroxynitrite and 300 mM morpholine at pH 7.5 as a function of added* HCO_3^-/CO_2. *T* 37°.

12). Now, **MorNO2** was already detected at 1 mM morpholine, and its maximum yield at 300 mM [**MorH**] had raised to *ca.* 150 μM. The yields of **MorNO** were less affected by air/CO_2 bubbling, levelling out at *ca.* 55 μM. These differences can be attributed to the reaction of morpholine with CO_2 to give morpholine carbamate [12], by this means depleting the CO_2 level in the solution if no extra CO_2 is supplied.

Peroxynitrite-Induced CIDNP Effects. To provide further support for the radical pathway of peroxynitrite-mediated formation of **MorNO** and **MorNO2**, ^{15}N-CIDNP studies were performed. ^{15}N-CIDNP Signals, *i.e.*, ^{15}N-NMR resonances of reaction products showing emission or enhanced absorption, unequivocally establish that these products are formed *via* radical pairs. Because the kinetic characteristics of peroxynitrite decay makes addition of preformed peroxynitrite to morpholine solutions unsuitable for CIDNP experiments, peroxynitrite was generated *in situ* at pH 4.5 by reaction of ^{15}N-labelled nitrite with H_2O_2. After addition of H_2O_2 (1M) to a mixture of $Na^{15}NO_2$ (0.25M), $NaHCO_3$ (0.05M), and morpholine (5M) in phosphate buffer (0.3M), four new major and one minor transient CIDNP signals were detected in the ^{15}N-NMR spectrum (*Fig. 13*,*a*). The signal at $\delta -29$ appeared in emission and has previously been identified to be due to ^{15}N-peroxynitric acid ($O_2{}^{15}NOOH$) [46–48]. A second emission signal at $\delta +11.5$ is very characteristic for *C*-nitroso compounds, hence tentatively attributed to a *C*-(^{15}N)nitrated morpholine product. The signals of $^{15}NO_3^-$ ($\delta -1.5$) and **Mor^{15}NO2** ($\delta -21$) showed enhanced absorption. Analogous effects of $^{15}NO_3^-$, $O_2{}^{15}NOOH$, and *C*-$^{15}NO_2$ have been observed during the reaction of *in situ* generated peroxynitrite with both tyrosine [11] and bovine albumine [49].

On the contrary, $^{15}NO_2^-$ (δ 232) and **Mor^{15}NO** (δ 146.7) were CIDNP-silent (signals not shown), hence, are not products of radical reactions. After completion of the reac-

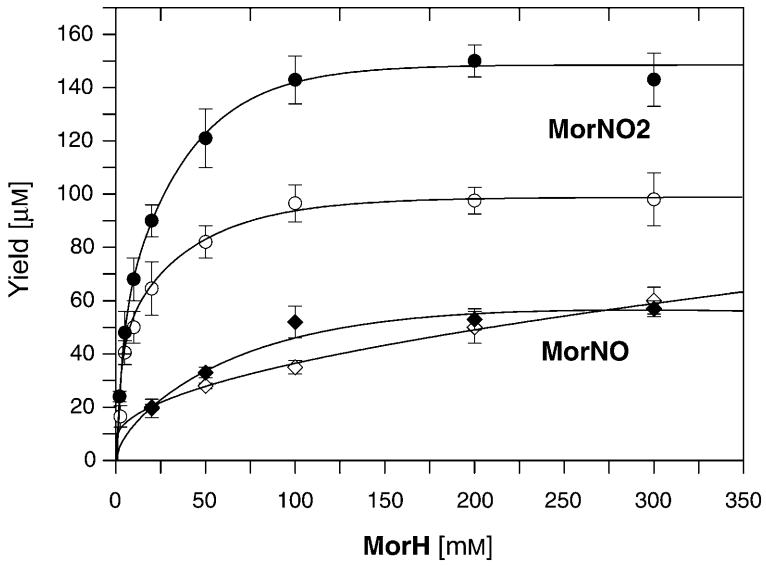

Fig. 12. N-*Nitroso- and* N-*nitromorpholine production from 1 mM peroxynitrite in the presence of 25 mM* HCO_3^-/CO_2 *as a function of the morpholine concentration: with additional flushing with air/*CO_2 (95 : 5%; black symbols) *and without additional flushing with air/*CO_2 (white symbols). *T* 37°.

tion, only $^{15}NO_3^-$ and **Mor^{15}NO** could be detected at normal gain. At higher gain, small signals of **Mor^{15}NO2** (δ −29) and a *C*-$^{15}NO_2$ compound (δ +11.5) became visible (*Fig. 13*, *b*), both corresponding to *ca.* 1% of all ^{15}N-labelled products. The ^{15}N-NMR resonance of $O_2{}^{15}NOOH$ was no longer observed, in accord with its limited lifetime ($t_{1/2}$ 30 min [46]) at this pH. It should be noted, however, that $O_2{}^{15}NOOH$ is not a unique intermediate in the presence of **MorH**, but rather is formed from further oxidation of peroxynitrous acid by excess H_2O_2 [46].

Formation of NO• and H_2O_2. In the presence of 25 mM HCO_3^-/CO_2, we were unable to detect at pH 7.5 any NO• released from 5 mM peroxynitrite, in accord with the effective trapping of peroxynitrite by CO_2. In the absence of morpholine, 4.3 ± 0.3 μM H_2O_2 were found after decomposition of 1 mM peroxynitrite at pH 7.5, *i.e.*, the same amount that was quantified in the absence of CO_2. After decomposition in the presence of 300 mM morpholine, the final H_2O_2 level had slightly increased to 9.3 ± 0.4 μM. Thus, H_2O_2 formation was suppressed by *ca.* 85% compared to the CO_2-free situation (see above).

3. Discussion. – *Reaction in the Absence of Carbon Dioxide.* The present investigation confirms the findings from three earlier reports [14][25][26] that both *N*-nitroso- (**MorNO**) and *N*-nitromorpholine (**MorNO2**) are produced from the reaction of peroxynitrite with morpholine (**MorH**) as a model compound for secondary amines. Nitrosoamine formation was also determined for some other secondary amines, showing that the yields of these products are dependent on pH, *i.e.*, related to the pK_as of the corresponding ammonium ions. However, in marked contrast to the above reports, we here demonstrate that *N*-hydroxymorpholine (**MorOH**) is in fact a major, at pH ≥ 7 the major product from the peroxynitrite–morpholine reaction over a wide range of pH

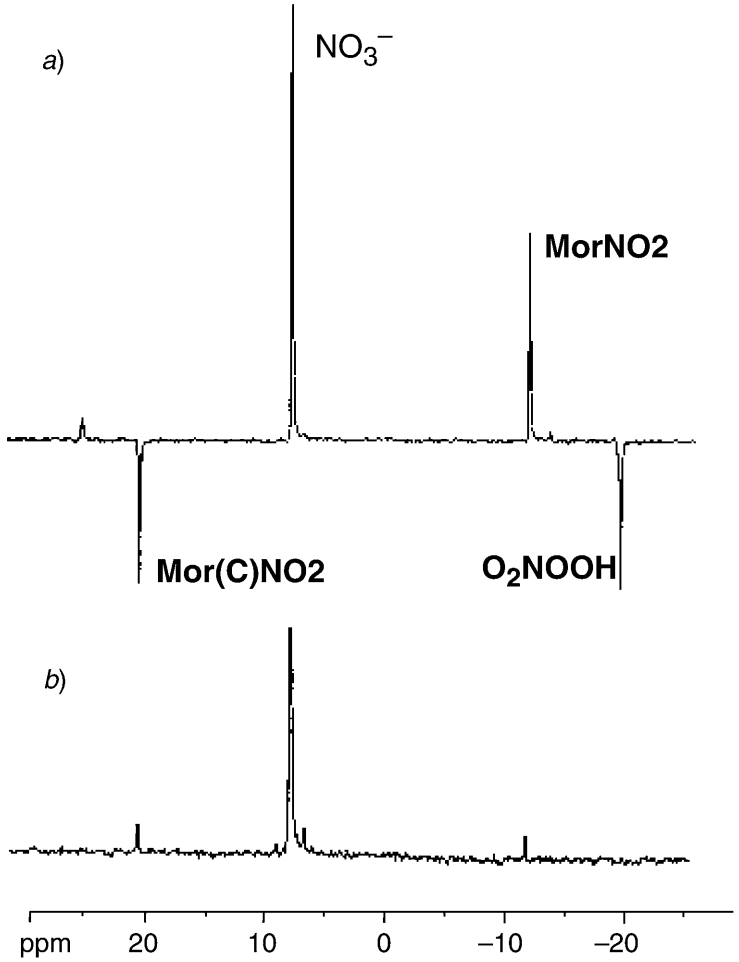

Fig. 13. *^{15}N-NMR Spectra from reaction of morpholine with* in situ *generated peroxynitrite at pH 4.5 in the presence of HCO_3^-/CO_2*, a) *recorded 1 min after mixing of the reactants, and* b) *recorded 1 h after mixing.* [**MorH**] = 1.0M, [$Na^{15}NO_2$] = 0.25M, [H_2O_2] = 1.0M, [$NaHCO_3$] = 0.05M, [phosphate buffer] = 300 mM; *T* 20°.

values. With regard to the fact that in the above cited papers product formation has been discussed in terms of a radical mechanism, with the intermediacy of the *N*-morpholinyl radical (**Mor**•), it is highly surprising that formation of **MorOH** has been overlooked or not even suspected[1]), because substantial O_2 production from peroxynitrite at pH > 6 has been shown before, and the very fast reaction of N- and C-centered rad-

[1]) This statement seems to be true for [26] and [14], whereas *Uppu*, *Squadrito*, and co-workers [25] in fact noted in a footnote that 'There might be minor products (arising from β-scission or other processes) from the reaction of **Mor**• with O_2 that we could not observe…'.

icals with O_2 is common knowledge. Generation of the morpholine-derived nitroxide radical (**MorO**$^{\bullet}$) in this system also has not been reported before. Hence, formation of oxygenated products must always be expected from reaction of peroxynitrite with organic substrates, even in the absence of atmospheric O_2, and, in fact, has frequently been observed.

MorOH formation is established here by ^{13}C-NMR spectroscopy (*Figs. 6, a–c*), which also indicates that **MorOH** is a 'direct' product from attack of peroxynitrite on **MorH**, *i.e.*, does not derive from further conversion of initially formed **MorNO** or **MorNO2**.

Formation of **MorOH**/**MorO**$^{\bullet}$ as well as the detection of a variety of morpholine-based by-products provides valuable insight into the mechanism by which peroxynitrite reacts with secondary amines. As noted in *Sect. 1*, there is overwhelming evidence for partial (*ca.* 28%) release of free (cage-escaped) HO$^{\bullet}$ and $^{\bullet}NO_2$ radicals during peroxynitrite decomposition (*Eqn. 1*). In the present system, the rather low yields of the detected morpholine-derived products, approaching constant values at high **MorH** concentrations, are fully explained by the combined action of these radicals. At the limiting **MorH** concentration of *ca.* 300 mM, the released HO$^{\bullet}$ radicals should react exclusively with morpholine. Due to their high reactivity, HO$^{\bullet}$ radicals may attack **MorH** at various positions, *i.e.*, by C–H and/or N–H H-atom abstraction (HAT) and/or by stepwise one-electron oxidation/deprotonation or proton-coupled electron transfer (PCET) at NH. To see what kind of intermediate(s) might preferably be produced, we estimated the thermochemistry of HO$^{\bullet}$ attack on unprotonated and protonated morpholine (*Eqns. 6* and *7*) by CBS-QB3 calculations. For the estimation of the free energies of reaction in aqueous solution, free energies of hydration were computed by utilizing the PCM-UAHF solvation model (*Table 4*).

$$C_4H_8NO + HO^{\bullet} \rightarrow C_4H_7NO^{\bullet} + H_2O \quad (6)$$

$$C_4H_9NO^{+} + HO^{\bullet} \rightarrow C_4H_8NO^{\bullet +} + H_2O \quad (7)$$

The data of *Table 4* show that the differences in the reaction energies for the four homolytic processes fall in a narrow range of just 5 kcal mol^{-1} in the gas phase as well as in aqueous solution. Since the driving forces are very similar, no reasonable conclusion can thus be drawn concerning a preferred pathway. The rates of HO$^{\bullet}$ attack are

Table 4. *CBS-QB3-Calculated Thermochemical Data* [kcal mol^{-1}] *for Hydrogen Abstraction from the Morpholine/Morpholinium Ion by Hydroxyl Radicals* (*Eqns. 6* and *7*).

Cleaved bond	$\Delta_r H^{\circ}$(g)[a])	$\Delta_r G^{\circ}$(g)[a])	$\Delta_r G^{\circ}$(aq)[b])	BDE[c])
H–N	–24.9	–26.1	–26.9	94.3[d])
H–C(3)	–26.6	–27.9	–29.0	92.5[e])
H–C(2)	–22.1	–23.4	–24.9	97.0
H–N^{+}(H)	–24.1	–25.2	–25.8	94.9

[a]) Gas phase. [b]) Aqueous phase, including hydration free energies calculated with the PCM-UAHF solvation model. [c]) Gas-phase bond-dissociation enthalpy (ΔH°). [d]) Exper.: 92.9 kcal mol^{-1} [73]. [e]) Exper.: 93.0 kcal mol^{-1} [73].

kinetically controlled, *i.e.*, may be governed by dissimilar intrinsic activation barriers for H-transfer, especially for the CH *vs.* NH moieties. (This issue has been addressed in a recent paper [50]). Nevertheless, since the largest energy difference is found for H-abstraction from the N- and O-bound CH_2 groups, the ^{13}C-NMR-detected by-products may thus be assumed to derive mainly from attack at the α-position with respect to the N-atom (*i.e.*, at C(3)) to give an α-aminoalkyl radical. With regard to the NH-derived products, we note that there is clear evidence that HO$^{\bullet}$ reacts with tertiary amines by one-electron transfer [24], and this likely happens as well with secondary amines, *i.e.*, with **MorH** [51]. The thus formed amine radical cation (**MorH**$^{\bullet+}$) would undergo rapid deprotonation, leading to the same intermediate *N*-morpholinyl radical (**Mor**$^{\bullet}$) as would be produced in a direct HAT process. Noteworthy, the computational data predict that NH H-abstraction from the morpholinium ion should also be feasible. However, there are many examples [30] establishing that HO$^{\bullet}$ reacts slower with protonated amines than it reacts with unprotonated ones (which in most cases react at the diffusion-controlled limit, $k = 10^9 - 10^{10}$ M^{-1} s^{-1}). Especially, abstraction of a H-atom from the ammonium group, *e.g.*, as shown in *Eqn. 8*, is a relatively slow reaction ($k_8 \approx 1 \cdot 10^6$ M^{-1} s^{-1}) [30].

$$(CH_3)_2NH_2^+ + {}^{\bullet}OH \rightarrow (CH_3)_2NH^{\bullet+} + H_2O \quad (8)$$

In agreement with this, overall conversion of **MorH** as well as production of **MorOH** is strongly diminished at pH 4.8 and enhanced at pH 9 compared to neutral conditions (*Fig. 6*). The lower rates for H-abstraction from protonated amines reflect the fact that the kinetics of HO$^{\bullet}$ reactions are influenced by pronounced *polar effects* (charge separation in the transition state), a consequence of the high electrophilicity of the HO$^{\bullet}$ radical. In conclusion, bond-dissociation enthalpies alone cannot be used to predict the (relative) rates of H-abstraction by such kind of radicals [50].

With consideration of the foregiong, the formation of **MorOH**, **MorO**$^{\bullet}$, and the minor by-products can be fully explained by the steps depicted in the *Scheme*. Attack of HO$^{\bullet}$ radicals on **MorH** either by HAT, PCET, or sequential one-electron transfer/deprotonation generates the morpholin-*N*-yl and the morpholin-2-yl radicals. Both radicals can safely be assumed to react diffusion-controlled ($k > 10^9$ M^{-1} s^{-1}) with O_2 (see [30][41] for leading reports) to yield the corresponding dioxy radicals. Along the upper pathway of the *Scheme*, the aminyldioxy radical then converts to the morpholin-*N*-yloxy radical **MorO**$^{\bullet}$. A related aminyldioxy radical from tetramethylpiperidine has recently been observed, and a mechanism for its conversion to the tetramethylpiperidine derived-nitroxide radical has been suggested [43]. It has been proposed that O_2 addition to the aminyl radical is a reversible process so that the aminyl radical may recombine with the aminyldioxy radical to give a highly unstable peroxide, which further breaks into two nitroxide radicals. Alternatively, the aminyldioxy radical may dimerize to an unstable tetroxide, which decomposes into two **MorO**$^{\bullet}$ and O_2. Considering the known decay mechanisms of nitroxide radicals, **MorOH** and the corresponding nitrone (= imine *N*-oxide) then should preferably be formed by disproportionation of **MorO**$^{\bullet}$. However, **MorOH** formation by H-transfer from an activated C–H bond cannot be excluded, since the decay of the EPR signals of **MorO**$^{\bullet}$ neither follows a clean second-order nor a clean first-order rate law (data not shown). This reaction

Scheme

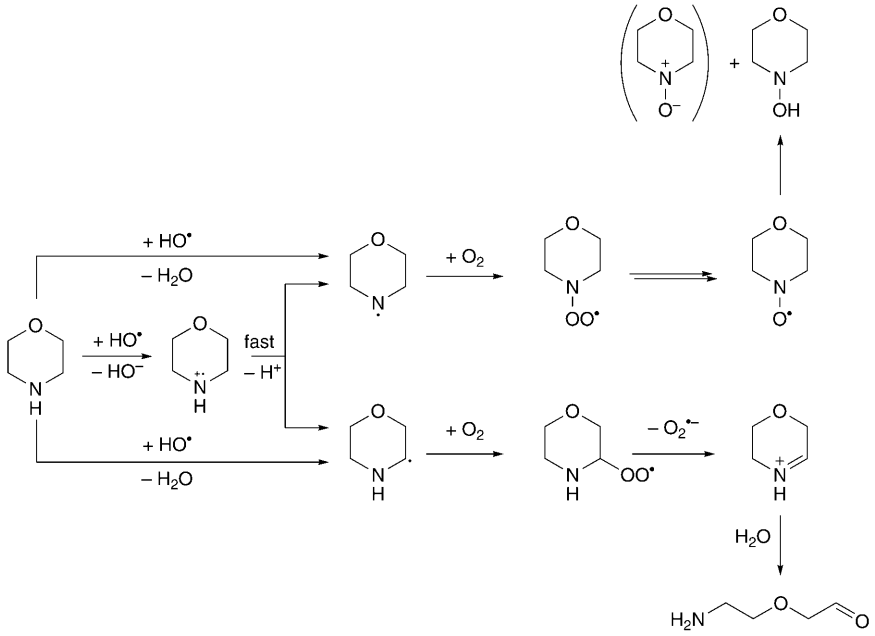

sequence is supported by the observation that the EPR signal of **MorO•** as well as the yield of **MorOH** are both enhanced by raising the pH from 7.5 to 9 (*Fig. 6*). The putative nitrone, or, a further reaction product of it, might be responsible for some of the observed minor CH_2 ^{13}C-NMR resonances. As peroxides are generally prone to nucleophilic attack by amines, leading to O–O bond cleavage, one might suspect that in the present system **MorOH** would be formed by such a nonradical process (*Eqn. 9*). However, this reaction can be excluded to play a significant role because of the low yield of **MorOH**, particularly at alkaline pH where the lifetime of peroxynitrite is strongly enhanced. Further, at pH 4.8, no additional formation of $^{15}NO_2^-$ could be detected by ^{15}N-NMR-spectrometry from ^{15}N-labelled peroxynitrite. It cannot be excluded, however, that a fraction of **MorOH** might be formed by attack of **Mor•** on peroxynitrite (*Eqn. 10*).

$$\mathbf{MorH} + ONOO^-/ONOOH \rightarrow \mathbf{MorOH} + NO_2^-/HNO_2 \quad (9)$$

$$\mathbf{Mor^\bullet} + ONOO^-/ONOOH \rightarrow \mathbf{MorO(^-)H} + NO_2^\bullet \quad (10)$$

Along the lower reaction path in the *Scheme*, rapid elimination of superoxide ($O_2^{\bullet -}$) from the α-aminodioxy radical is feasible (see [41] for leading reports) to give the corresponding cyclic iminium ion/imine, which further might be hydrolyzed to a ring-opened aldehyde. This prototypal reaction would explain part of the aldehyde-type signals as well as some of the CH_2 resonances observed in the ^{13}C-NMR spectrum (*Fig. 6*). The formation of hydrogen peroxide (*Fig. 9*) *via* dismutation of superoxide (*Eqn. 11*) is also in line with such a reaction.

$$2\ O_2^{\bullet-} + 2\ H^+ \rightarrow H_2O_2 + O_2 \quad (11)$$

Of course, in an oxidizing environment such as the present one, the reactions outlined in the *Scheme* cannot fully describe all peroxynitrite-dependent alterations on morpholine, and a variety of side reactions, *e.g.*, starting from the depicted radical intermediates, are expected. The several observed carbonyl ^{13}C-NMR resonances strongly indicate that oxidative opening of the morpholine ring proceeds at other positions, too. Additional, ring-opened products may also be expected from oxidative attack on the 'early' products, *e.g.*, **MorNO** [52]. Noteworthy, no monosubstituted morpholine-derived products were detected in the ^{13}C-NMR spectra, indicating that such compounds are rapidly further oxidized and/or easily decomposed by hydrolysis [52].

With regard to the proposed intermediacy of **Mor**$^{\bullet}$, the formation of **MorNO** has been explained by *Uppu*, *Squadrito*, and co-workers [25], and *Ohshima* and co-workers [26] by the recombination of peroxynitrite-released nitric oxide with **Mor**$^{\bullet}$. However, the fact that the detectable production of $^{\bullet}$NO from peroxynitrite (in the absence of any other substrate) is only 0.4% renders the formation of **MorNO** by this recombination reaction highly unlikely. Alternatively, one might, in analogy to *Eqn. 9*, propose that peroxynitrite would act as a direct, electrophilic nitrosating agent (*Eqn. 5*).

In fact, *van der Vliet* and co-workers [19] speculated that the peroxynitrite-dependent formation of *S*-nitrosoglutathione occurs by such a process, although no satisfying evidence has been presented. However, the limiting, low yields of **MorNO** (*Figs. 1* and *4*) at high **MorH** concentrations in conjunction with the observation that there is no correlation between formation of **MorNO** and of H_2O_2 (*Fig. 9*) safely rules out that **MorNO** is produced *via* such a process. Rather, the intermediacy of a peroxynitrite-derived nitrosating species, which can be completely trapped at high morpholine concentrations, is indicated. Of course, at pH 4.5, either N_2O_3 or HNO_2, formed from NO_2^- are expected to be the major nitrosating intermediates. At pH $\geq$ 7, where the concentration of NO_2^- (*ca.* 150 μM) is given by the contamination (15 mol-%) of the peroxynitrite stock solution, the formation of these nitrosating species can be ignored. Furthermore, the inhibitory effect of azide on the peroxynitrite-mediated formation of **MorNO** (*Fig. 7*) cannot solely be related to the scavenging of N_2O_3, because low azide concentrations even slightly increase nitrite production from peroxynitrite (*Fig. 8*). In addition, the significant nitrosation of morpholine at pH 11 (*Fig. 4*) disproves both HNO_2 and N_2O_3 as major nitrosating species, because the latter entity is rapidly terminated by OH^- ($k(N_2O_3 + OH^-) = 2 \cdot 10^3 + 10^8 [OH^-]\ s^{-1}$ [53]). The inhibitory effect of azide can be reasonably explained by the reaction sequence of *Eqns. 12–16*.

$$ONOOH \rightarrow {}^{\bullet}OH + {}^{\bullet}NO_2 \quad (12)$$

$$N_3^- + {}^{\bullet}OH \rightarrow OH^- + {}^{\bullet}N_3 \quad (13)$$

$${}^{\bullet}N_3 + ONOO^- \rightarrow N_2 + N_2O + O_2^{\bullet-} \quad (14)$$

$$O_2^{\bullet-} + {}^{\bullet}NO_2 \rightarrow O_2NOO^- \quad (15)$$

$$O_2NOO^- \rightarrow O_2 + NO_2^- \quad (16)$$

According to this sequence, azide is expected to down-regulate the concentration of nitrogen dioxide which exists in equilibrium with its dimer N_2O_4, a potent nitrosating species [32][54][55]. The radical terminating capabilities of azide in the peroxynitrite/CO_2/**MorH** system has previously been emphasized by *Uppu*, *Squadrito*, and coworkers [25], who stated that '…N_3^- acts as a general free-radical quencher rather than as a specific scavenger of NO^+ carriers'. N_2O_4 is well-known to *N*-nitrosate secondary aliphatic amines even at alkaline pH [56]. As peroxynitrous acid in part fragmentizes to hydroxyl radical and nitrogen dioxide (*Eqn. 1*), N_2O_4 will be produced. Thus, N_2O_4 should be the major nitrosating entity in our system. This conclusion is strongly supported by the effect of azide on the yield of nitrate and nitrite (*Fig. 8*) as well as by the fact that the [**MorNO**]/[**MorNO2**] product ratio of 4–5 is typical for the action of N_2O_4 [57]. Thus, formation of carcinogenic *N*-nitrosoamines must generally be expected when peroxynitrite decays in the presence of secondary amines.

In the absence of CO_2, the yield of **MorNO2** is low (1.6 mol-% relative to applied peroxynitrite). We found no evidence for its formation *via* recombination of **Mor**$^\bullet$ with $NO_2^\bullet$. Instead, it was observed that the yield of **MorNO2** increases at alkaline pH (*Fig. 6*) at the expense of both **MorNO** (*Fig. 3*) and H_2O_2 (*Fig. 9*). Therefore, we propose that part of **MorNO2** is generated from an electrophilic attack of N_2O_4 on morpholine in addition to oxidation of **MorNO** with H_2O_2 [58].

Reaction in the Presence of Carbon Dioxide. In the presence of CO_2, peroxynitrite generates carbonate radicals ($CO_3^{\bullet-}$) with a yield of *ca.* 30–33% at the expense of $^\bullet$OH (*Eqn. 17*) [7–9]. As a consequence of this reaction, the production of both NO_2^- and O_2 from peroxynitrite is strongly decreased because the HO$^\bullet$ can no longer attack $ONOO^-$ effectively. The $CO_3^{\bullet-}$ radical ($E^\circ(CO_3^{\bullet-}/CO_3^{2-}=1.5$ V) [59] is, as compared to HO$^\bullet$ (E°(HO$^\bullet$/$OH^-=1.9$ V, $E^\circ(H^+,{}^\bullet OH/OH_2=2.72$ V) [59], a weaker oxidant but is nevertheless expected to oxidize morpholine (*Eqn. 18*) (*e.g.*, $CO_3^{\bullet-}$ reacts moderately fast with piperazine ($k=3\cdot10^6$ M^{-1} s^{-1}) [30]), thereby also producing the aminyl and the α-aminoalkyl radicals similarly to the paths shown in the *Scheme* for HO$^\bullet$. The decisive difference to the CO_2-free situation lies in the fact that peroxynitrite does not release significant amounts of O_2 in the presence of CO_2 [4], so that now $NO_2^\bullet$ can effectively compete with the dissolved atmospheric O_2 (if any) for the morpholine-derived radicals. The latter assumption is supported by the fact that the yield of H_2O_2 from the peroxynitrite–morpholine reaction is reduced by *ca.* 85% on adding HCO_3^-/CO_2 to the reaction mixture and, of course, by the emission characteristic of the resonance of 3-nitromorpholine in the ^{15}N-NMR CIDNP spectrum (*Fig. 13*). Recombination of the C-centered morpholinyl radical with freely diffusing $NO_2^\bullet$ builds up a so-called *F-pair* which collapses to 3-nitromorpholine producing an emission (*E*) signal (*Eqn. 19*).

$$ONOO^- + CO_2 \rightleftharpoons ONOOCO_2^- \rightleftharpoons [O_2{}^{15}N^\bullet;{}^{\bullet-}O_3C]_{cage} \xrightarrow{30-33\%} {}^\bullet NO_2 + CO_3^{\bullet-} \quad (17)$$

$$CO_2 + NO_3^-$$

$$CO_3^{\bullet-} + \mathbf{MorH} \rightarrow \mathbf{MorH}^{\bullet+} + CO_3^{2-} \quad (18)$$

$$^{\bullet}{}^{15}NO_2 + {}^{\bullet}C(3)\mathbf{Mor} \rightarrow [O_2{}^{15}N^{\bullet};{}^{\bullet}C(3)\mathbf{Mor}]^F \rightarrow 3\text{-}{}^{15}NO_2\mathbf{MorH}\ (E) \quad (19)$$

Most interestingly, the resonance of **MorNO2** exhibits enhanced absorption (*A*) during reaction, and this CIDNP effect cannot be produced by recombination of freely diffusing $NO_2^{\bullet}$ radicals with **Mor**$^{\bullet}$ radicals. Since the pK_a value of the morpholinium ion is 8.5 at 25° [60] and because the pK_a value of nonaromatic aminium radical ions ($R_2NH^{\bullet+}$) are generally 2–3 pH units lower than those of the corresponding ammonium ions ($R_2NH_2^+$) [61][62], a pK_a value in the range of 5.5–6.5 is expected for **MorH**$^{\bullet+}$. Since the CIDNP experiments had to be performed with *in situ* generated peroxynitrite at pH 4.5, **MorH**$^{\bullet+}$ rather than **Mor**$^{\bullet}$ should be the free N-centered radical that reacts with $NO_2^{\bullet}$. As aliphatic aminium ions are highly reactive in H-transfer processes [62], their lifetime should be extremely short at the applied high morpholine concentration of 300 mM. Thus, recombination of **MorH**$^{\bullet+}$ with nitrogen dioxide is strongly disfavored. Even though, such a reaction would lead to an emission (*E*) signal in the ^{15}N-NMR spectrum of **MorNO2**. The observed enhanced absorption (*A*) signal of **MorNO2** thus can be only explained by the occurrence of a cage-substitution reaction, thereby building up radical *S-pairs* (*Eqns. 20* and *21*).

$$[O_2{}^{15}N^{\bullet};{}^{\bullet-}O_3C]^S + \mathbf{MorH} \rightarrow [\mathbf{MorH}^{+\bullet};{}^{\bullet}{}^{15}NO_2]^S + CO_3{}^{2-} \quad (20)$$

$$[\mathbf{MorH}^{\bullet+};{}^{\bullet}{}^{15}NO_2]^S \rightarrow \mathbf{MorNO2}\ (A) + H^+\ (\text{cage reaction}) \quad (21)$$

At pH ≥ 7, however, it is expected that the morpholine-derived aminyl radical recombines with nitrogen dioxide to yield **MorNO2**. From the yields of **MorNO2** and **MorNO** at such pH values, *i.e.*, 15 and 5.5% relative to peroxynitrite (*Fig. 12*), we can conclude that the peroxynitrite-derived yield of free $^{\bullet}NO_2$ must be in the range of *ca.* 26%, in good agreement with earlier reports [7–9].

We are grateful to *Heinz Bandmann* (Universität Duisburg-Essen) for the NMR measurements.

Experimental Part

Materials. Peroxynitrite ($ONOO^-$) stock solns. (710 ± 20 mM) were prepared as described previously [24]. **MorOH** and **MorNO2** were prepared by standard procedures [63][58]. All other compounds and solvents were commercially available. $Na^{15}NO_2$ labelled with 99.3% ^{15}N (*Isotec Inc.*) was employed. Care was taken to exclude possible contamination by transition metals by treating the buffer solns. with the heavy-metal-scavenger resin *Chelex-100* [24]. For easy ^{13}C- and ^{15}N-NMR identification of the peroxynitrite–morpholine reaction products, a mixture of **Mor^{15}NO**, **Mor^{15}NO2**, and **MorOH** was prepared by electrolysis (Pt electrode, 2 cm^2; current density 25–30 mA cm^{-2}; 4 h) of a mixture of $Na^{15}NO_2$ (1M) and morpholine (1M) in a rapidly stirred biphasic aq. KOH soln. (pH 13)/CH_2Cl_2 1:1 (*v/v*) (30 ml) system according to *Evtyugin et al.* [64]. After separation of the org. layers, the aq. phase was extracted with CH_2Cl_2 (3×), the org. phases were combined, and the solvent was evaporated at 0°. ^{13}C-NMR Analysis (CD_3CN) showed a *ca.* 4:2:1 molar ratio of the above compounds. ^{13}C-NMR (CD_3CN): *Table 2*. ^{15}N-NMR (MeCN, ext. standard $Me^{15}NO_2$): 153.2 (**Mor^{15}NO**); −23.4 (**Mor^{15}NO2**); small amounts of $^{15}NO_3^-$ at −3.3 and of $^{15}NO_2^-$ at 233.2; no other ^{15}N-labelled compounds were detected. The spectral assignments are in accord with literature data [65–67].

CE Measurements. **MorOH**, **MorNO**, **MorNO2**, and the nitrosamines of 'diethanolamine', piperidine, and pyrrolidine were quantified by capillary-zone electrophoresis (CE) on a *Beckman-P/ACE-*

5000 apparatus under the following conditions: fused silica capillary (effective length 50 cm, internal diameter 75 μm), hydrodynamic injection for 5 s, *T* 30°, voltage 20 kV, normal polarity, UV detection at 254 nm. As electrolyte system, a mixture of 20 mM sodium phosphate and 100 mM sodium dodecyl sulfate (pH 6.45) was used. To each sample, 1 mM *N*-nitrosodimethylamine was added as internal standard. Nitrate and nitrite were quantified as described previously [4].

NMR Measurements. ^{13}C- and ^{15}N-NMR Spectra: *Bruker-DRX-500* spectrometer; at 125.7 and 50.7 MHz, resp. ^{13}C-NMR: acquisition by collecting 16 transients; δ(C) rel. to $SiMe_4$ (= 0 ppm). ^{15}N-NMR: rel. to (^{15}N)nitromethane (= 0 ppm) as external standard. Reaction of peroxynitrous acid with morpholine was carried out by adding aliquots of the alkaline peroxynitrite stock soln. under vortexing to 300 mM solns. of **MorH** in the buffer soln. to give a final concentration of 10 mM peroxynitrite. D_2O was added as internal lock (H_2O/D_2O 9:1), and the mixture was transferred to 5-mm NMR tubes.

EPR Measurements. EPR Spectra: *Bruker-ESP-300E*-X-band spectrometer (*Bruker,* Rheinstetten, Germany), equipped with a TM_{110} wide-bore cavity; at 20°. Solns. were prepared from 2 ml of the phosphate buffer soln. (pH 7.4) containing morpholine (300 mM). Aliquots of the alkaline (pH 14) stock soln. of peroxynitrite were added to the morpholine soln. by vortexing under aerobic and anaerobic conditions to give the desired concentrations. The mixtures were quickly transferred to a 0.4-mm aq.-soln. quartz cell (*Willmad*, Buena, N.J., USA). The first spectra were run as fast as possible, *i.e.*, within 1 min after mixing. Instrument settings: microwave frequency 9.8 GHz, microwave power 20 mW, sweep range 100 G, sweep time 4 min, and modulation amplitude 1 G, unless otherwise indicated. Standard spectral simulations were carried out with the WinSim program [68][69], exchanged-broadenend spectra were simulated with the EPREXN program [70][71].

CIDNP Measurements. The ^{15}N-CIDNP experiments were performed as reported before [11][49][47]. The mixtures were prepared in 10-mm NMR tubes by adding 1M H_2O_2 to solns. of $Na^{15}NO_2$ (0.05M) in H_2O/D_2O 9:1 containing phosphate buffer (0.3M) and $NaHCO_3$ (0.05M). The pH was adjusted with H_2SO_4 and NaOH. During reaction, the pH decreased by about half a pH unit because of the formation of nitric acid. The pH values given in *Fig. 13* refers to the initial pH after mixing of the reactants. The tubes were quickly transferred into the probe head of the ^{15}N-NMR spectrometer (*Bruker DPX-300*) and locked within 1 min after mixing of the reactants (internal lock: D_2O). The ^{15}N-NMR spectra were then taken by using single pulses with pulse angles of 90°. Chemical shifts are given in δ values relative to (^{15}N)nitromethane dissolved in MeCN as an external reference.

Quantum-Chemical Calculations. Complete Basis Set (CBS-QB3) computations were carried out with the Gaussian 03 suite of programs [72]. *Gibbs* free energies of solvation for water were estimated for the optimized gas-phase geometries with the PCM-UAHF procedure incorporated in Gaussian 03. Both the PCM/(U)HF/6-31+G(d) and the CBS-QB3 methodology are known to provide estimates within 'chemical accuracy' ($\pm$1 kcal mol^{-1}).

REFERENCES

[1] J. S. Beckman, T. W. Beckman, J. Chen, P. A. Marshall, B. A. Freeman, *Proc. Natl. Acad. Sci. U.S.A.* **1990**, *87*, 1620.
[2] S. V. Lymar, J. K. Hurst, *Chem. Res. Toxicol.* **1998**, *11*, 714.
[3] C. E. Richeson, P. Mulder, V. W. Bowry, K. U. Ingold, *J. Am. Chem. Soc.* **1998**, *120*, 7211.
[4] M. Kirsch, H.-G. Korth, A. Wensing, R. Sustmann, H. de Groot, *Arch. Biochem. Biophys.* **2003**, *418*, 133.
[5] Y. Zhao, K. N. Houk, L. P. Olson, *J. Phys. Chem. A* **2004**, *108*, 5864.
[6] V. P. Tret'yakov, L. A. Min'ko, E. S. Rudakov, *Theor. Exp. Chem.* **2004**, *40*, 309.
[7] S. V. Lymar, J. K. Hurst, *J. Am. Chem. Soc.* **1995**, *117*, 8867.
[8] S. Goldstein, G. Czapski, J. Lind, G. Merenyi, *Chem. Res. Toxicol.* **1999**, *12*, 132.
[9] M. G. Bonini, R. Radi, G. Ferrer-Sueta, A. M. D. C. Ferreira, O. Augusto, *J. Biol. Chem.* **1999**, *274*, 10802.
[10] H. Ischiropoulos, L. Zhu, J. Chen, M. Tsai, J. C. Martin, C. D. Smith, J. S. Beckman, *Arch. Biochem. Biophys.* **1992**, *298*, 431.
[11] M. Lehnig, *Arch. Biochem. Biophys.* **1999**, *368*, 303.

[12] M. Kirsch, H.-G. Korth, R. Sustmann, H. de Groot, *Chem. Res. Toxicol.* **2000**, *13*, 451.
[13] B. Alvarez, H. Rubbo, M. Kirk, S. Barnes, B. A. Freeman, R. Radi, *Chem. Res. Toxicol.* **1996**, *9*, 390.
[14] K. Kikugawa, K. Hiramoto, T. Ohkawa, *Biol. Pharm. Bull.* **2004**, *27*, 17.
[15] N. Nonoyama, H. Oshima, C. Shoda, H. Suzuki, *Bull. Chem. Soc. Jpn.* **2001**, *74*, 2385.
[16] M. Kirsch, M. Lehnig, *Org. Biomol. Chem.* **2005**, *3*, 2085.
[17] M. A. Moro, V. M. Darley-Usmar, D. A. Goodwin, N. G. Read, R. Zamora-Pino, M. Feelisch, M. W. Radomski, S. Moncada, *Proc. Natl. Acad. Sci. U.S.A.* **1994**, *91*, 6702.
[18] B. Mayer, A. Schrammel, P. Klatt, D. Koesling, K. Schmidt, *J. Biol. Chem.* **1995**, *270*, 17355.
[19] A. van der Vliet, P. A. Chr. 't Hoen, P. S.-Y. Wong, A. Bast, C. E. Cross, *J. Biol. Chem.* **1998**, *273*, 30255.
[20] T. Suzuki, H. F. Mower, M. D. Friesen, I. Gilbert, T. Sawa, H. Ohshima, *Free Radic. Biol. Med.* **2004**, *37*, 671.
[21] M. Kirsch, H. de Groot, *J. Pineal Res.* **2006**, *40*, 10.
[22] N. Nonoyama, K. Hisatome, C. Shoda, H. Suzuki, *Tetrahedron Lett.* **1999**, *40*, 6939.
[23] R. M. Uppu, W. A. Pryor, *J. Am. Chem. Soc.* **1999**, *121*, 9738.
[24] M. Kirsch, E. E. Lomonosova, H. G. Korth, R. Sustmann, H. de Groot, *J. Biol. Chem.* **1998**, *273*, 12716.
[25] R. M. Uppu, G. L. Squadrito, R. M. Bolzan, W. A. Pryor, *J. Am. Chem. Soc.* **2000**, *122*, 6911.
[26] M. Masuda, H. F. Mower, B. Pignatelli, I. Celan, M. D. Friesen, H. Nishino, H. Ohshima, *Chem. Res. Toxicol.* **2000**, *13*, 301.
[27] M. Kirsch, H. de Groot, *J. Biol. Chem.* **2000**, *275*, 16702.
[28] M. Kirsch, M. Lehnig, H.-G. Korth, R. Sustmann, H. de Groot, *Chem.–Eur. J.* **2000**, *7*, 3313.
[29] M. Kirsch, H. de Groot, *FASEB J.* **2001**, *15*, 1569.
[30] A. B. Ross, W. G. Mallard, W. P. Helman, G. Buxton, V. R. E. Huie, P. Neta, 'NDRL/NIST Solution Kinetics Database 3.0', NDRL/NIST, Gaithersburg, MD, 1998.
[31] S. Goldstein, A. Saha, S. V. Lymar, G. Czapski, *J. Am. Chem. Soc.* **1998**, *120*, 5549.
[32] D. L. H. Williams, 'Nitrosation Reactions and the Chemistry of Nitric Oxide', Elsevier, Amsterdam, 2004.
[33] S. Goldstein, G. Czapski, *J. Am. Chem. Soc.* **1998**, *120*, 3458.
[34] M. Bätz, H.-G. Korth, P. Meineke, R. Sustmann, *Methods Enzymol.* **1998**, *301*, 532.
[35] P. Meineke, U. Rauen, H. de Groot, H.-G. Korth, R. Sustmann, *Chem.–Eur. J.* **1999**, *5*, 1738.
[36] P. Meineke, U. Rauen, H. de Groot, H.-G. Korth, R. Sustmann, *Biol. Chem.* **2000**, *381*, 575.
[37] 'Landolt-Börnstein, New Series. Radical Reaction Rates in Liquids', Ed. H. Fischer, Springer, Berlin, 1983, 1984, Vol. II/13a,b.
[38] O. Augusto, R. M. Gatti, R. Radi, *Arch. Biochem. Biophys.* **1994**, *310*, 118.
[39] S. Dikalov, M. Skatchkov, E. Bassenge, *Biochem. Biophys. Res. Commun.* **1997**, *231*, 701.
[40] H. Karoui, N. Hogg, C. Frejaville, P. Tordo, B. Kalyanaraman, *J. Biol. Chem.* **1996**, *271*, 6000.
[41] C. von Sonntag, H. P. Schuchmann, *Angew. Chem., Int. Ed. Engl.* **1991**, *30*, 1229.
[42] K. U. Ingold, J. R. Roberts, *J. Am. Chem. Soc.* **1973**, *95*, 3288.
[43] H. A. Göttinger, V. E. Zubarev, O. Brede, *J. Chem. Soc., Perkin Trans. 2* **1997**, 2167.
[44] J. J. Windle, J. A. Kuhnle, B. H. Beck, *J. Chem. Phys.* **1969**, *50*, 2630.
[45] A. Hudson, H. A. Hussain, *J. Chem. Soc. B* **1968**, 251.
[46] E. H. Appelman, D. J. Gosztola, *Inorg. Chem.* **1995**, *34*, 787.
[47] M. Lehnig, M. Kirsch, H.-G. Korth, *Inorg. Chem.* **2003**, *42*, 4275.
[48] M. Lehnig, M. Kirsch, *Org. Biomol. Chem.* **2006**, *4*, 721.
[49] M. Lehnig, K. Jakobi, *J. Chem. Soc., Perkin Trans. 2* **2000**, 2016.
[50] P. Mulder, H. G. Korth, K. U. Ingold, *Helv. Chim. Acta* **2005**, *88*, 370.
[51] O. Brede, D. Beckert, C. Windolph, H. A. Göttinger, *J. Phys. Chem. A* **1998**, *102*, 1457.
[52] H.-J. Kim, J. C. Fishbein, *Chem. Res. Toxicol.* **2003**, *16*, 715.
[53] A. Treinin, E. Hayon, *J. Am. Chem. Soc.* **1970**, *92*, 5821.
[54] D. L. H. Williams, *NITRIC OXIDE: Biol. Chem.* **1997**, *1*, 522.
[55] M. Kirsch, H.-G. Korth, R. Sustmann, H. de Groot, *Biol. Chem.* **2002**, *383*, 389.
[56] B. C. Challis, S. A. Kyrtopoulos, *J. Chem. Soc., Perkin Trans. 1* **1978**, 299.

[57] B. C. Challis, S. A. Kyrtopoulos, *J. Chem. Soc., Perkin Trans. 1* **1978**, 1296.
[58] W. D. Emmons, A. F. Ferris, *J. Am. Chem. Soc.* **1953**, *75*, 4623.
[59] D. M. Stanbury, *Adv. Inorg. Chem.* **1989**, *33*, 69.
[60] H. B. Hetzer, R. G. Bates, R. A. Robinson, *J. Phys. Chem.* **1966**, *70*, 2869.
[61] R. W. Fessenden, P. Neta, *J. Phys. Chem.* **1972**, *76*, 2857.
[62] Y. L. Chow, W. C. Dauen, S. F. Nelsen, D. H. Rosenblatt, *Chem. Rev.* **1978**, *78*, 243.
[63] E. R. Blout, S. G. Cohen, M. Green, U.S. Pat. 2843481, 1958, p. 1–4.
[64] G. A. Evtyugin, V. U. Gol'frid, D. A. Semanov, V. Z. Latypova, Y. M. Kargin, L. N. Punegova, G. A. Marchenko, *J. Gen. Chem. USSR (Engl. Transl.)* **1989**, *59*, 2497.
[65] B. C. Challis, T. I. Yousaf, *J. Chem. Soc., Chem. Commun.* **1990**, 1598.
[66] Y.-D. Park, H.-K. Kim, J.-J. Kim, S.-D. Cho, S.-K. Kim, M. Shiro, Y.-J. Yoon, *J. Org. Chem.* **2003**, *68*, 9113.
[67] M. Witanowski, L. Stefaniak, G. A. Webb, *Annu. Rep. NMR Spectrosc.* **1993**, *25*, 468.
[68] D. R. Duling, 'WinSim', Laboratory of Molecular Biophysics, NIEHS, NIH, Research Triangle Park, North Carolina, 1994.
[69] D. R. Duling, *J. Magn. Reson. B* **1994**, *104*, 105.
[70] J. Heinzer, 'EPREXN', ETH Zürich, 1971.
[71] J. Heinzer, *Mol. Phys.* **1971**, *22*, 167.
[72] M. J. Frisch, G. W. Trucks, H. B. Schlegel, G. E. Scuseria, M. A. Robb, J. R. Cheeseman, J. A. Montgomery Jr., T. Vreven, K. N. Kudin, J. C. Burant, J. M. Millam, S. S. Iyengar, J. Tomasi, V. Barone, B. Mennucci, M. Cossi, G. Scalmani, N. Rega, G. A. Petersson, H. Nakatsuji, M. Hada, M. Ehara, K. Toyota, R. Fukuda, J. Hasegawa, M. Ishida, T. Nakajima, Y. Honda, O. Kitao, H. Nakai, M. Klene, X. Li, J. E. Knox, H. P. Hratchian, J. B. Cross, C. Adamo, J. Jaramillo, R. Gomperts, R. E. Stratmann, O. Yazyev, A. J. Austin, R. Cammi, C. Pomelli, J. W. Ochterski, P. Y. Ayala, K. Morokuma, G. A. Voth, P. Salvador, J. J. Dannenberg, V. G. Zakrzewski, S. Dapprich, A. D. Daniels, M. C. Strain, O. Farkas, D. K. Malick, A. D. Rabuck, K. Raghavachari, J. B. Foresman, J. V. Ortiz, Q. Cui, A. G. Baboul, S. Clifford, J. Cioslowski, B. B. Stefanov, G. Liu, A. Liashenko, P. Piskorz, I. Komaromi, R. L. Martin, D. J. Fox, T. Keith, M. A. Al-Laham, C. Y. Peng, A. Nanayakkara, M. Challacombe, P. M. W. Gill, B. Johnson, W. Chen, M. W. Wong, C. Gonzalez, J. A. Pople, 'Gaussian 03, Revision C.02', Gaussian Inc., Pittsburgh PA, 2003.
[73] D. D. M. Wayner, K. B. Clark, A. Rauk, D. Yu, D. A. Armstrong, *J. Am. Chem Soc.* **1997**, *119*, 8925.

Received April 28, 2006